RESEARCH PAPER

Synthesis and Characterization of Ru (III)-Doped Magnetic Manganese Ferrite Nanoparticles

Dunia Butrus Toma Al-Bakzo [1], *Mohanad Y. Saleh* [1]* *and Shakir Mahmood Saied* [2]

[1] *Department of Chemistry, College of Education for Pure Science, University of Mosul, Mosul, Iraq*
[2] *College of Pharmacy, Al-Noor University, Mosul, Iraq*

ARTICLE INFO

Article History:
Received 01 July 2026
Accepted 21 August 2026
Published 01 October 2026

Keywords:
BET analysis
Ruthenium Catalyst
TGA analysis
VSM analysis
XRD analysis

ABSTRACT

Effect of ruthenium (Ru) doping on magnetic properties of manganese ferrite nanoparticles ($MnFe_2O_4$ MNPs) with the composition $Ru_{0.3}MnFe_{1.7}O_4$ were prepared by chemical co-precipitation and further thermally treated at 300, 600 and 900 °C where the annealing temperature is systematically studied through structural, morphological, textural, thermal and magnetic properties characterizations. X-ray diffraction (XRD) analysis verified the cubic spinel ferrite phase in addition to changes in crystallinity as a function of annealing temperature. $Ru_{0.3}MnFe_{1.7}O_4$ MNPs was characterized using various spectroscopic instruments, confirming the characteristic metal-oxygen vibrations of the spinel structure with Fourier transform infrared spectroscopy (FTIR). Particle morphology and aggregation were analyzed using scanning electron microscopy (SEM). Subsequently, the elemental composition was verified via energy-dispersive X-ray spectroscopy (EDX) and inductively coupled plasma optical emission spectroscopy (ICP-OES). Thermogravimetric analysis (TGA) testified on thermal stability. In addition, Brunauer-Emmett-Teller (BET) analysis was used to probe the porosity present within the assembled nanoparticles. Vibrating sample magnetometry (VSM) results were also collected for measurements of the magnetic saturation. Thus, these results as a whole demonstrate that Ru doping combined with thermal annealing make it possible to tailor both the structural and magnetic properties of manganese ferrite nanoparticles rendering them to be promising materials for soft magnet applications as well as magnetically responsive materials.

How to cite this article
Al-Bakzo D., Saleh M., Saied S. Synthesis and Characterization of Ru (III)-Doped Magnetic Manganese Ferrite Nanoparticles. J Nanostruct, 2026; 16(4):5200-5208. DOI: 10.22052/JNS.2026.04.058

INTRODUCTION

Recently, due to tunable magnetic and electrical properties, ferrite-based materials have gained much attention for many modern applications [1,2]. These materials are widely used in magnetic resonance imaging (MRI), targeted drug delivery systems, data storage devices, and other biomedically relevant applications [3,4]. In the biomedical fields, MNPs encapsulated by appropriate carriers can be directed inside the human body using an external magnetic field to specifically target cancerous tissues [5]. Ferrites can be either soft or hard magnetic materials depending on composition and microstructure, with the corresponding physical property dependence very temperature sensitive [6].

* Corresponding Author Email: mohanadalallaf@uomosul.edu.iq

Among the spinel ferrites, manganese ferrite ($MnFe_2O_4$) MNPs has recently gained attention as a but promising candidate due to its structural stability, tunable magnetic properties, where it is $MnFe_2O_4$ exists in a spinel crystal structure, with magnetic properties highly dependent on the equilibrium fraction of Mn^{2+} and Fe^{3+} cation distribution between tetrahedral (A) and octahedral (B) sites in its formula AB_2O_4 [7-9]. The magnetic behavior of $MnFe_2O_4$ MNPs originated from the imbalance between the magnetic moments at A and B sublattices, while dielectric response is due to carrier hopping, interfacial polarization and grain boundary effects [10,11]. Dielectric constant and dielectric loss in ferrites are strongly affected by frequency, temperature, and the synthesis route, so these factors should be carefully considered when ferrite-based materials are designed for biomedical, magnetic, and electronic-related applications. Although spinel ferrites have been widely studied, the doping of $MnFe_2O_4$ MNPs with transition-metal or rare-earth elements still deserves more attention, because this modification can change cation distribution within the spinel lattice and influence magnetic exchange interactions, electrical conductivity, and relaxation behavior [12-15]. Such effects are also associated with particle size, crystallinity and surface morphology, each of which can be manipulated using desired synthesis and heat-treatment conditions [16].

Ru is a transition metal with good catalytic activity and excellent electrical conductivity, which can also be used as doping to adjust the physical behavior of some magnetic nanoparticles such as spinel ferrites [17,18]. Doping $MnFe_2O_4$ with transition metals, such as Fe, Co, Zn and Ru has been shown to influence cation redistribution within the spinel lattice followed by magnetic exchange interactions that can improve the magnetic performance of different devices [19-21]. Such changes are desirable for some applications, like magnetic recording media and electronic devices that require low coercivity with moderate dielectric loss and stable magnetic response [22-24]. Nickel [25], Palladium [26], Zinc [27], and Iron [28] can be used to synthesize magnetic catalysts attached to graphene oxide. These catalysts exhibit physical changes depending on the temperature, and temperature variations affect the proportions of these elements [29,30]. These catalysts can also be used to increase the adsorption of charcoal and multiply the amount of material that can be removed or adsorbed, such as dyes or pollutants [31]. Herein, $Ru_{0.3}MnFe_{1.7}O_4$ MNPs were synthesized via a simple co-precipitation method, which leads up to the synthesis of homogenous ferrite materials. The samples prepared were crushed and subsequently subjected to different annealing temperatures (300, 600, and 900 °C) in order to analyze the influence of the thermal treatment on their structure, morphology, magnetic characteristics and dielectric-related properties.

MATERIALS AND METHODS

All chemicals and reagents used in this study were purchased from Merck and Fluka and used without further purification. The synthesized materials were characterized using Fourier-transform infrared spectroscopy, (SEM)Scanning Electron Microscopy, (EDX)Energy-dispersive X-ray spectroscopy, (TGA)Thermogravimetric analysis, (XRD)X-Ray Diffraction, and (VSM) techniques/ Vibrating-sample magnetometer.

Synthesis of $MnFe_2O_4$ MNPs

The co-precipitation method was used to synthesize $MnFe_2O_4$ nanoparticles, with manganese chloride hexahydrate ($MnCl_2$) (4 mmol) and ferric chloride ($FeCl_3$) (8 mmol) as the starting materials. To stimulate precipitation, a 0.1 M aqueous sodium hydroxide solution was added to the mixture (chlorine metal salts) in deionized water with continuous stirring until homogeneity was achieved. The resulting product was then heated at 80 °C for two hours. Magnetic separation was used to separate the product, followed by washing with deionized water and ethanol. The drying process was carried out using a convection oven at 80 °C [32].

Synthesis of $Ru_{0.3}MnFe_{1.7}O_4$ MNPs

$Ru_{0.3}MnFe_{1.7}O_4$ MNPs were prepared by incorporating Ru^{3+} into the pre-synthesized $MnFe_2O_4$ MNPs. The as-prepared $MnFe_2O_4$ MNPs were dispersed in distilled water and ultrasonicated for 30 min to obtain a homogeneous mixture. Then the required stoichiometric amount of $RuCl_3$ was dissolved separately in distilled water and then added to the $MnFe_2O_4$ MNPs suspension under continuous magnetic stirring. The mixture was stirred for 12 h to ensure uniform distribution of Ru^{3+} ions over the ferrite surface. After that freshly an aqueous solution of $NaBH_4$ was added drop by drop with continuous stirring to reduce (Ru^{+3} to $Ru^{0)}$ at room temperature (r.t.) [33]. After that the resulting solid product was magnetically separated, washed several times with distilled water to remove residual ions and reaction by-products, and dried at 100 °C for 24 h The dried material was finely ground and calcined in an electric oven at 300, 600 and 900 °C for two hours.

RESULTS AND DISCUSSION

In this work, $MnFe_2O_4$ MNPs were used as the substrate. Ru was then introduced into the $MnFe_2O_4$ MNPs to modify its structural and functional properties. After synthesis, the prepared $Ru_{0.3}MnFe_{1.7}O_4$ MNPs underwent heat treatment at temperatures of 300, 600, and 900 °C. Several characterization techniques were employed. FT-IR was used, XRD was used to examine the phase composition and crystallinity. The morphology and properties of the particles were studied using SEM. Also was used EDX, ICP-OES, BET and TGA.

FT-IR spectra

The FT-IR spectrum of $Ru_{0.3}MnFe_{1.7}O_4$ nanoparticles (Fig. 1) exhibits a broad absorption band in the range 3300-3200 cm^{-1} attributed to O-H stretching vibrations of surface hydroxyl groups and adsorbed moisture. The absorption band at 1630 cm^{-1} is assigned to H-O-H bending vibrations of adsorbed water molecules, respectively [34]. Furthermore, the characteristic bands appearing at 560-583 cm^{-1} and 439 cm^{-1} correspond to metal-oxygen stretching vibrations at the tetrahedral and octahedral sites, respectively, confirming the formation of the cubic spinel structure of Manganese ferrite [35].

XRD analysis

Fig. 2 presents the X-ray diffraction (XRD) patterns of $Ru_{0.3}MnFe_{1.7}O_4$ MNPs annealed in air at 300, 600, and 900 °C for 2 h. All diffraction peaks can be indexed to the cubic spinel structure of Manganese ferrite (JCPDS card No. 10-0319) [36]. The prominent reflections observed at 2θ

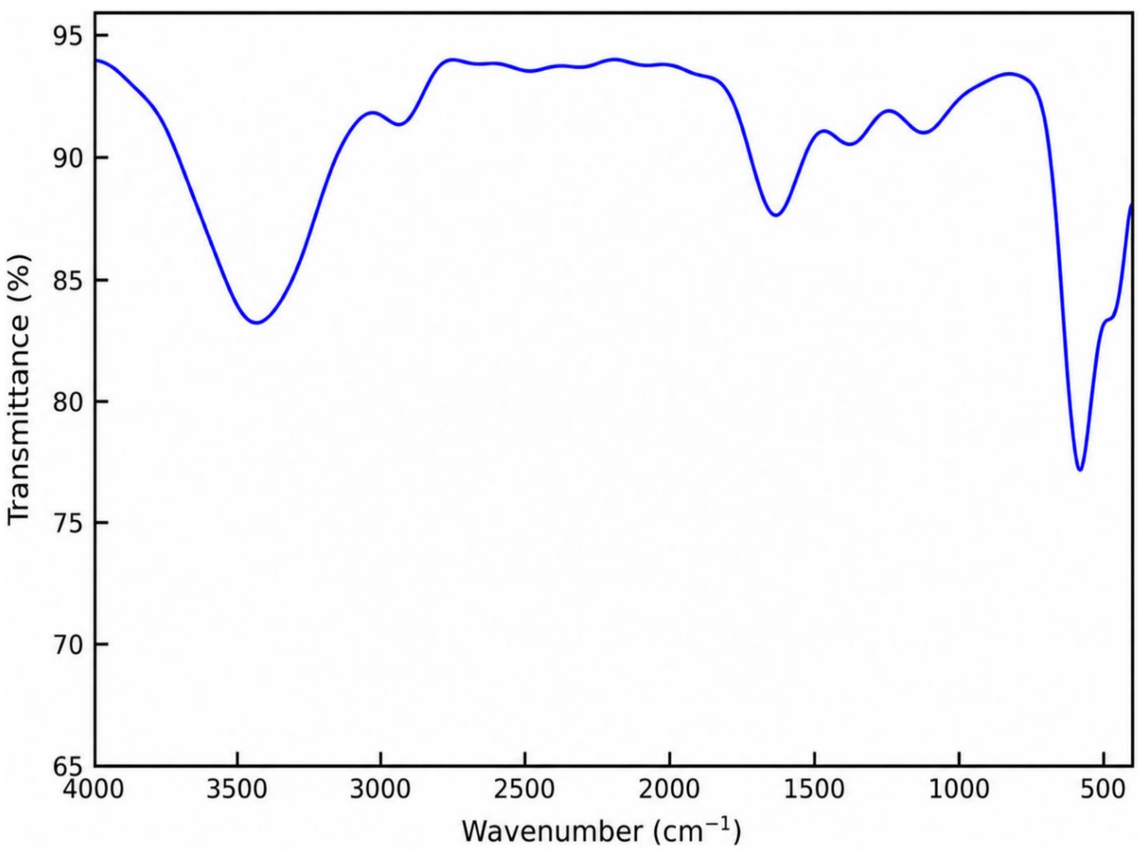

Fig. 1. FT-IR spectrum of $Ru_{0.3}MnFe_{1.7}O_4$ MNPs.

values of approximately 18.4°, 29.8°, 35.1°, 39.1°, 44.2°, 53.1°, 56.5°, 62.3°, and 74.1° correspond to the (111), (220), (311), (400), (422), (511), (440), and (533) crystallographic planes, respectively, confirming the formation of a face-centered cubic spinel phase. As the annealing temperature increases, the diffraction peaks become sharper and more intense, indicating improved crystallinity and grain growth [37-39].

SEM analysis

The SEM micrographs of $Ru_{0.3}MnFe_{1.7}O_4$ MNPs depicted in (Fig. 3 a-c) for the particular at 300 °C, 600 °C, and 900 °C, respectively. The particles are found to have unique clumping and non-uniform shapes after heat treatment at 300 °C, as well as relatively uneven sizes indicating incomplete crystal growth. At 600 °C, moderate morphological changes are observed, but the distribution and size of the particles are more homogeneous than in the first stage. At 900 °C, more distinctly shaped and larger particles are observed, with greater clumping, possibly due to increased calcination and further particle maturation [40, 41].

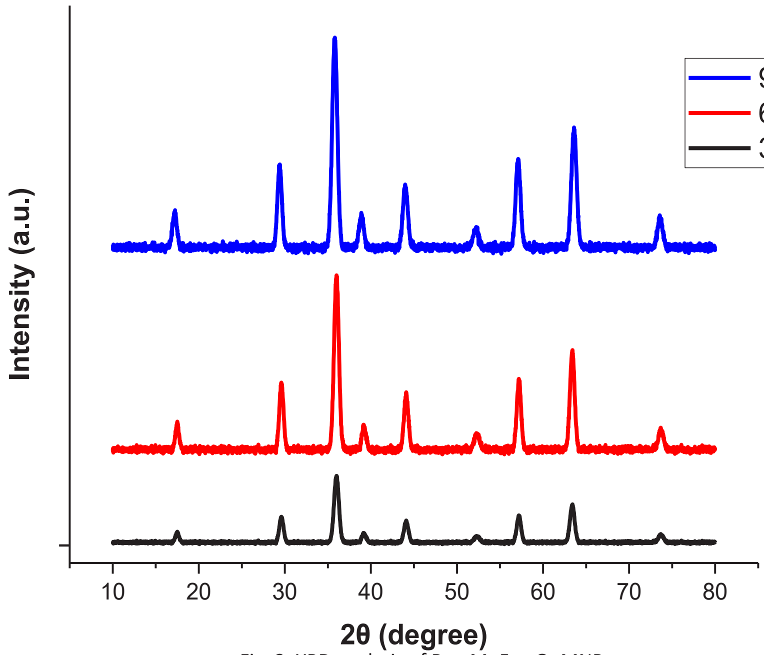

Fig. 2. XRD analysis of $Ru_{0.3}MnFe_{1.7}O_4$ MNPs.

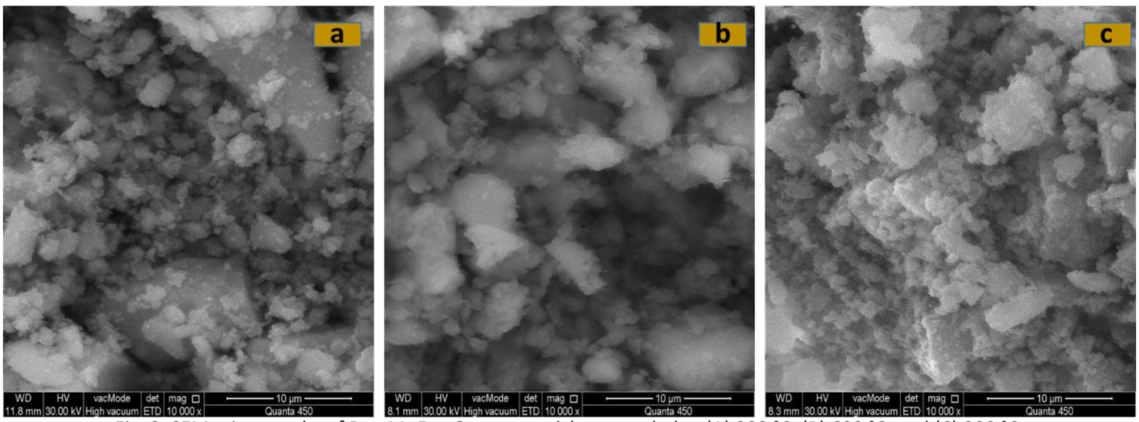

Fig. 3. SEM micrographs of $Ru_{0.3}MnFe_{1.7}O_4$ nanoparticles annealed at (A) 300 °C, (B) 600 °C, and (C) 900 °C.

EDX analysis

The EDX spectrum of $Ru_{0.3}MnFe_{1.7}O_4$ MNPs confirms the presence of Ru, Mn, Fe, and O (Fig. 4). The absence of other peaks indicates good chemical purity and conformity to the desired chemical composition. Elemental mapping images are shown in Fig. 5, demonstrating a homogeneous distribution without any noticeable segregation or agglomeration. Furthermore, ICP-OES measurements of the larger samples revealed a Ru content of approximately 12.5 wt%, consistent with the expected composition of $Ru_{0.3}MnFe_{1.7}O_4$ MNPs, thus confirming the high retention of Ru during the $MnFe_2O_4$ synthesis.

VSM analysis

The magnetic saturation value was measured using VSM analysis at room temperature for

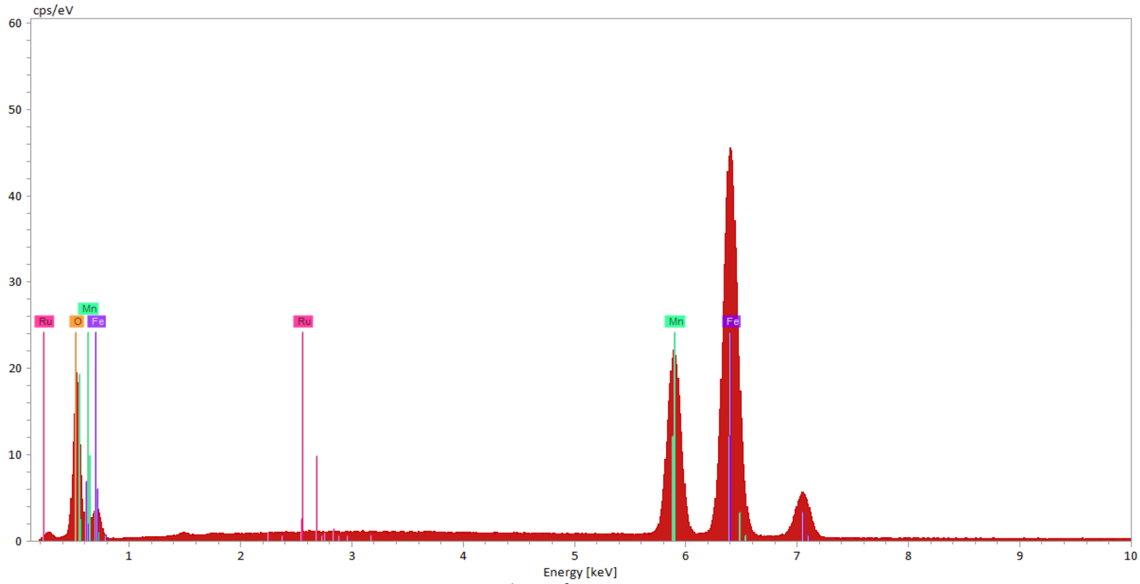

Fig. 4. EDX analysis of $Ru_{0.3}MnFe_{1.7}O_4$ MNPs.

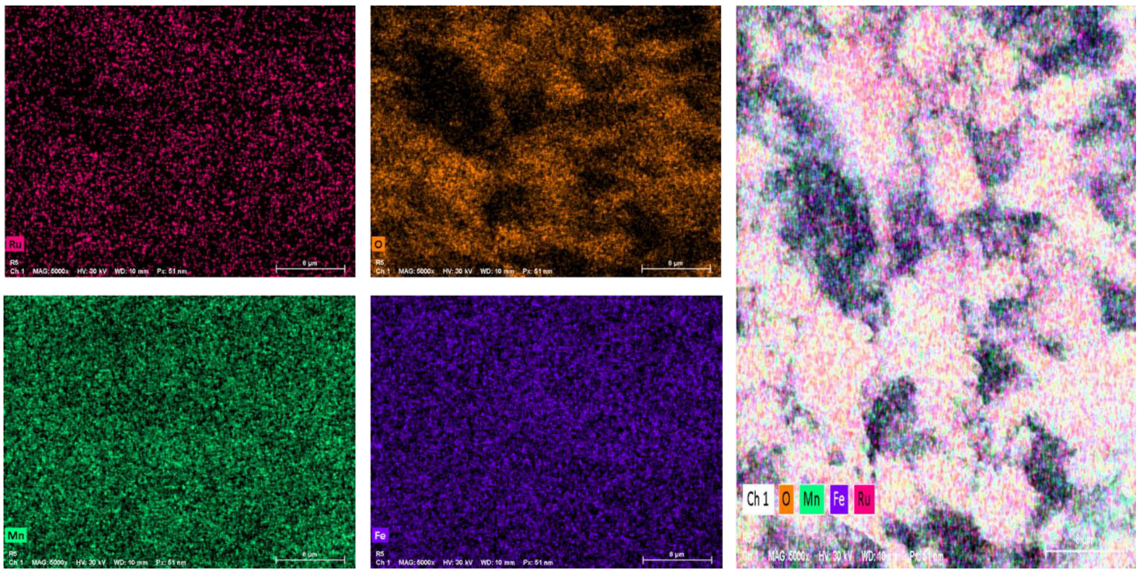

Fig. 5. EDX elemental mapping images of $Ru_{0.3}MnFe_{1.7}O_4$ MNPs.

the $Ru_{0.3}MnFe_{1.7}O_4$. Fig. 6 shows the magnetic hysteresis curves of $Ru_{0.3}MnFe_{1.7}O_4$ annealed at (300, 600 and 900 °C). The narrow hysteresis loops of all samples also indicate the soft magnetic properties. The values of saturation magnetization systematically increase with the increase of annealing temperature, about 34 emu g^{-1} for a sample treated at 900 °C. This trend matches the increase in crystallinity and grain growth at higher annealing temperatures, as this can diminish lattice defects and surface spin disorder [42,43]. With increasing crystallization, the magnetic ordering of the spinel lattice improves and obtains stronger magnetic exchange interactions. The presence of fairly narrow loops also implies low coercivity, but precise coercivity and remanence values can only be determined with careful examination of the low-field region. It was concluded that the VSM results confirm the significant influence of annealing temperature on the magnetic response

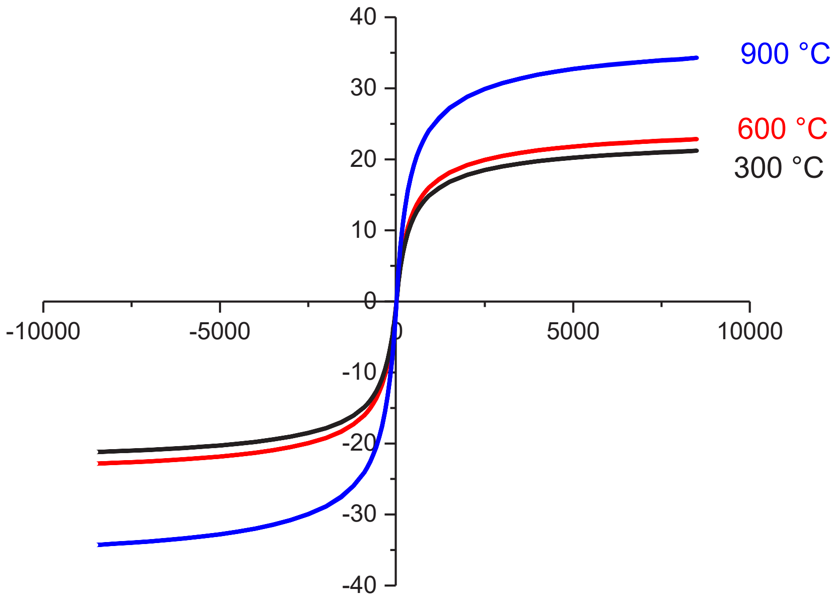

Fig. 6. VSM analysis of $Ru_{0.3}MnFe_{1.7}O_4$ MNPs.

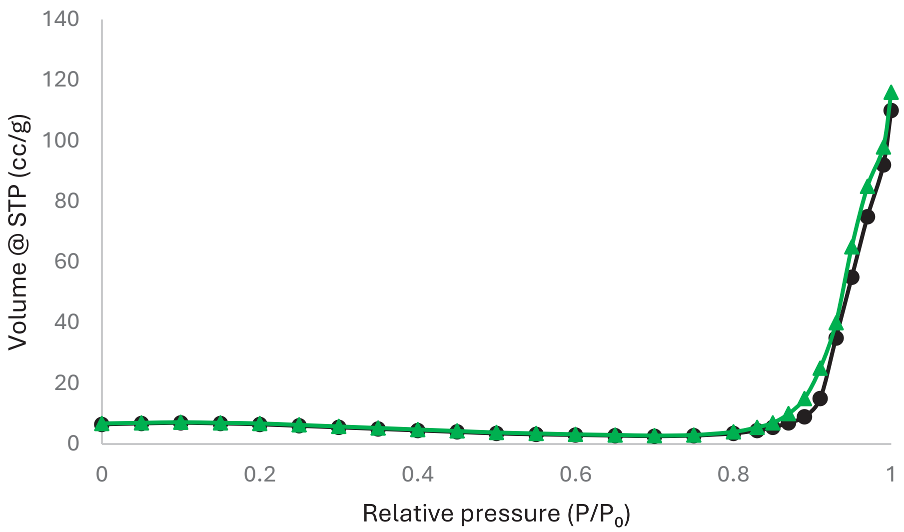

Fig. 7. BET analysis of $Ru_{0.3}MnFe_{1.7}O_4$ MNPs.

of $Ru_{0.3}MnFe_{1.7}O_4$ MNPs.

BET analysis

N_2 adsorption-desorption isotherm of $Ru_{0.3}MnFe_{1.7}O_4$ MNPs. As shown in Fig. 7, $Ru_{0.3}MnFe_{1.7}O_4$ MNPs display a type IV profile with significant hysteresis loop at high relative pressure and thereby show the mesoporous property. Only a small amount of adsorption at low P/P_0 may indicate insignificant contribution from micropores, while the large increase in adsorbed volume within the interval of 0.85-1.0 is mainly related to capillary condensation taking place mostly inside mesopores and between neighboring particles. The texture of this porosity is related to the intrinsic characteristics that magnetic ferrite nanoparticles have, which tend to self-aggregate due to their high surface energy and consequently generate more surfaces with potential interactions between them. The hysteresis loop is characteristic of the H3 type, indicating that slit-like pores are generated between irregularly packed nanoparticles rather than uniformly tubular structures. Additionally, the lack of a defined plateau at or near saturation also reinforces open mesoporous structures. On the other hand, these open pores can enhance surface accessibility and mass transfer of $Ru_{0.3}MnFe_{1.7}O_4$ MNP.

TGA analysis

The thermogravimetric curve of $Ru_{0.3}MnFe_{1.7}O_4$ MNPs. The TGA curve displayed in Fig. 8 demonstrates a continuous weight loss within the studied temperature range, confirming that this prepared ferrite material exhibits good thermal stability. The weight loss below 150 °C is attributable to the removal of physically adsorbed water and residual surface moisture. Significant mass loss between 150 and 380 °C mainly due to the disproportionation of chemically bonded water, surface hydroxyl groups and some possible unwashed speciation products from co-precipitation. After 400 °C, the curve tends to level off essentially, with just relatively small extra weight loss up to 700 °C indicating the completion of major decomposition processes and augmentation of a thermally stable $Ru_{0.3}MnFe_{1.7}O_4$ MNPs. The weight loss is not significant, decreasing from about 99-100% to nearly 91%, which corresponds to an overall mass loss of approximately 8-9% [44]. This small loss demonstrates that $Ru_{0.3}MnFe_{1.7}O_4$ MNPs possess

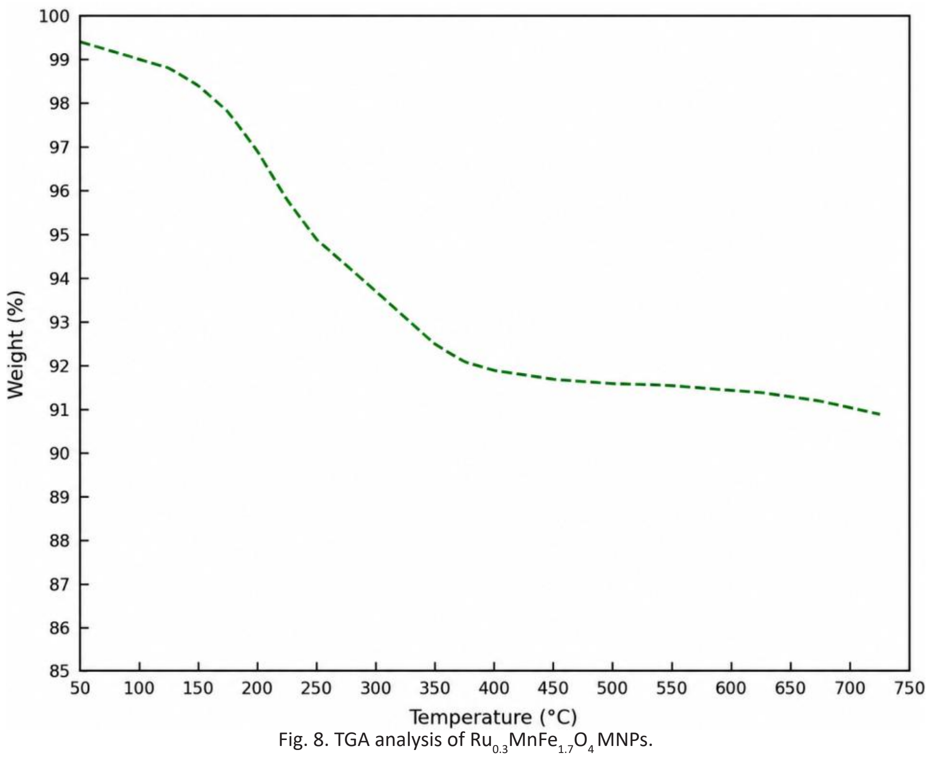

Fig. 8. TGA analysis of $Ru_{0.3}MnFe_{1.7}O_4$ MNPs.

good thermal stability. At an elevated temperature, the tiny change in residual mass may be attributed to further dehydroxylation, elimination of trace impurities or stabilization/unsaturation of lattice structural defects occurring during thermal treatment. Thus, the results from TGA show that these nanoparticles have a significant structural stability under high temperature.

The combined results of the tests reveal that the overall outcome of ruthenium doping with thermal annealing makes it possible to engineer both the structural and magnetic properties of manganese ferrite nanoparticles, making them promising materials for soft magnet applications as well as magnetically responsive materials. The effect of temperature on the synthesis of the nanocatalyst is structurally significant, as it showed a marked improvement in catalyst properties with increasing temperature.

The importance of the above catalyst could be very high if used as an adsorbent for compounds that cause environmental pollution or interfere with dyes, among other important applications.

CONCLUSION

This study demonstrates that Ru-doped manganese ferrite nanoparticles can be prepared as thermally stable and magnetically responsive oxide nanomaterials through a modified co-precipitation route followed by controlled annealing. The incorporation of ruthenium into the manganese ferrite system offers a useful strategy for tuning the spinel ferrite framework and improving its functional behavior. The prepared nanoparticles showed characteristics that make them suitable for applications requiring stable soft magnetic materials. Future studies should focus on accurately correlating the actual Ru loading with cation distribution, magnetic interactions, and practical performance in catalytic, adsorption, or electromagnetic applications.

CONFLICT OF INTEREST

The authors declare that there is no conflict of interests regarding the publication of this manuscript.

REFERENCES

1. Ali R, Hussein SA, Znad MR, Al-Delfi MN. Applications of Nano Magnesium Ferrite as a Catalyst in the Preparation of Heterocyclic Compounds: A Short Review. Chemistry Africa. 2025;8(3):839-853.
2. Kazemi M. Based on $CuFe_2O_4$ MNPs: Magnetically recoverable nanocatalysts in coupling reactions. Synth Commun. 2020;50(14):2114-2131.
3. Ali R, Murad AH, Al sultani Z. Probiotic Supplementation: A Promising Preventive Strategy for Dental Caries. Future Dental Research. 2024;2(1):19-30.
4. Mohammadi Z, Montazerabadi A, Irajirad R, Attaran N, Abedi H, Mousavi Shaegh SA, et al. Optimization of cobalt ferrite magnetic nanoparticle as a theranostic agent: MRI and hyperthermia. Magn Reson Mater Phys, Biol Med. 2023;36(5):749-766.
5. Abdel Maksoud MIA, Ghobashy MM, Kodous AS, Fahim RA, Osman AI, Al-Muhtaseb AaH, et al. Insights on magnetic spinel ferrites for targeted drug delivery and hyperthermia applications. Nanotechnology Reviews. 2022;11(1):372-413.
6. Jalili H, Aslibeiki B, Hajalilou A, Musalu O, Ferreira LP, Cruz MM. Bimagnetic hard/soft and soft/hard ferrite nanocomposites: Structural, magnetic and hyperthermia properties. Ceram Int. 2022;48(4):4886-4896.
7. Kalaivani S, Marichamy P, Sakunthala A, Shadap M. Synergistic integration of $MnFe_2O_4$ and biochar for enhanced supercapacitive performance: structural, electrochemical, and stability insights. Ionics. 2025;32(1):987-1010.
8. Giribaldi A, Divakaran AM, Maltoni P, Rijckaert H, Latronico G, Piscino C, et al. Effect of the Deposition Temperature on the Properties of $MnFe_2O_4$ Thin Films. Elsevier BV; 2026. http://dx.doi.org/10.2139/ssrn.6304352
9. Lázaro JPM, Cruz-López E, Palafox-Corona A, Navarrete-Prieto DA. $MnFe_2O_4$ nanoparticles for VOCs sensing application at low operating temperature. Elsevier BV; 2026. http://dx.doi.org/10.2139/ssrn.6145980
10. Nancy, Thakur P, Verma R, Kumar D, Das DR, Sun AC, et al. Calcium-doped manganese nanoferrites via hydrothermal synthesis: correlation of structure, electrical conductivity, and electrochemical performance. Appl Phys A. 2026;132(3).
11. Sánchez-León Y, Briceño S. Electrical conduction mechanism of cobalt-modified $MnFe_2O_4$ ferrites nanoparticles. J Magn Magn Mater. 2026;652:174164.
12. Inam S, Khalid M, Uddin Z, Younas M, Boukhris I, Ashiq MGB. Magneto-electric properties of (1-x)$LaFeO_3$ - (x) $MnFe_2O_4$ based hybrid nanocomposites for advanced technological applications. Surfaces and Interfaces. 2025;72:107070.
13. Amjad M, Bibi I, Iqbal M, Kamal S, Mustafa G, Nouren S, et al. Interfacial coupling-driven enhancement of capacitance in $MnFe_2O_4$/NiO nanocomposites synthesized via sol–gel auto-combustion. J Sol-Gel Sci Technol. 2026;117(3).
14. Dippong T, Levei EA, Petean I, Deac IG, Cadar O. A Strategy for Tuning the Structure, Morphology, and Magnetic Properties of $MnFe_2O_4/SiO_2$ Ceramic Nanocomposites via Mono-, Di-, and Trivalent Metal Ion Doping and Annealing. Nanomaterials. 2023;13(14):2129.
15. Aslibeiki B, Kameli P, Salamati H, Concas G, Salvador Fernandez M, Talone A, et al. Co-doped $MnFe_2O_4$ nanoparticles: magnetic anisotropy and interparticle interactions. Beilstein Journal of Nanotechnology. 2019;10:856-865.
16. Judith Vijaya J, Sekaran G, Bououdina M. Effect of Cu^{2+} doping on structural, morphological, optical and magnetic properties of MnFe2O4 particles/sheets/flakes-like nanostructures. Ceram Int. 2015;41(1):15-26.
17. Wang H, Abruña HD. Comparative Study of Ru-Transition Metal Alloys and Oxides as Oxygen Evolution Reaction Electrocatalysts in Alkaline Media. ACS Applied Energy

Materials. 2022;5(9):11241-11253.
18. Xu W, Huang H, Wu X, Yuan Y, Liu Y, Wang Z, et al. Mn-doped Ru/RuO_2 nanoclusters@CNT with strong metal-support interaction for efficient water splitting in acidic media. Composites Part B: Engineering. 2022;242:110013.
19. Rahman MU, Khan RA, Khan AM, Sreearunothai P, Qurratulain R, Noor U, et al. Fabrication of Co/Zn Doped Manganese Ferrite Magnetic Nanoparticles: Improving Electrochemical Detection of Antibiotic Through Modification of Reduced Graphene Oxide. Journal of Inorganic and Organometallic Polymers and Materials. 2024;35(4):2943-2961.
20. Yoon S. Structural and magnetic investigation of Fe-doped $Mn_{3-x}Fe_xO_4$ (x≤ 0.1). AIP Advances. 2026;16(2).
21. Nanjappan M, Rajagopalan H, Elaiyaraja P, Athikesavan V, Nandisha PS. Co-doping in manganese ferrite nanoparticles: tailoring structural, electrical, and magnetic properties for visible light-driven enhanced catalytic dye degradation applications. Journal of Materials Science: Materials in Electronics. 2025;36(29).
22. Dumitru I, Caltun OF. Ferrites use in magnetic recording. Ferrite Nanostructured Magnetic Materials: Elsevier; 2023. p. 733-745. http://dx.doi.org/10.1016/b978-0-12-823717-5.00017-6
23. Gupta S, Wei C-Y, Tai N-H. Composition tunable manganese-doped magnetite microwave absorber composites for radio frequency identification communication. Ceram Int. 2022;48(11):15105-15115.
24. Ansari SM, Phase D, Kolekar YD, Ramana CV. Effect of Manganese-Doping on the chemical and optical properties of cobalt ferrite nanoparticles. Materials Science and Engineering: B. 2024;300:117134.
25. Kuryazov R, Thalij K, Aldulaimi A, Saleh MY, Almehizia AA, Buzrukov T, et al. Development of a novel GO/Fe@TANG composite electrode for green and sustainable electrosynthesis of N -phenylbenzamides via electrocatalytic carbonylation and hydrogenation. New J Chem. 2026;50(1):557-584.
26. Saied SM, Mohammed SJ, Khaleel BT, Saleh MY. Comparative studies between conventional techniques and green chemistry to synthesis of novel piperidinium salts ionic liquids (PBSILs).
27. Hassan EM, Saleh MY, Saied SM, Kazemi M. Magnetic-MOF Zinc nanocatalyst in DESs Solvent: a sustainable route for 2,4-Disubstituted Quinoline synthesis. J Organomet Chem. 2025;1040:123812.
28. Saleh MY, Sadeek GT, Saied SM. Preparation and characterization of a dual acidic Ionic Liquid functionalized Graphene Oxide nanosheets as a Heterogeneous Catalyst for the Synthesis of pyrimido [4, 5-b] quinolines in water. Iranian Journal of Catalysis. 2023;13(4).
29. Mohammed Abdulrazaq M, Noor HMS. A comparative study of the theoretical and practical values of ionization constants for amino acid derivatives in the neutral and anionic states. Applied Chemical Engineering. 2025.
30. Saeed NHM, Ali RT, Saied SM. Computational study on the Estramustine (EMCYT) and its active metabolites anticancer drugs 17-α-estradiol and nornitrogen. Results in Chemistry. 2025;18:102747.
31. Hasb AMA, Saeed NHM. Chlorination Of N-Benzoyl Valine By Sodium N-Chloro-Para-Toluene Sulfonyl Amide (Cat) Hydrochloric Acidic: A Kinetic And Mechanism Study. Chemical Problems. 2025;23(2):239-248.
32. Wang W-W. Microwave-induced polyol-process synthesis of $MIIFe_2O_4$ (M=Mn, Co) nanoparticles and magnetic property. Materials Chemistry and Physics. 2008;108(2-3):227-231.
33. Karataş Y, Zengin A, Gülcan M. Pd-doped flower like magnetic $MnFe_2O_4$ spinel ferrit nanoparticles: Synthesis, structural characterization and catalytic performance in the hydrazine-borane methanolysis. Journal of the Energy Institute. 2023;110:101360.
34. Nady H, Ali IO, Alenezy EK, Salama EE, Salama TM, Elhenawy AA, et al. Structural and vibrational characteristics of $MnFe_2O_4$ spinal ferrites for electrochemical hydrogen evolution reaction. J Sol-Gel Sci Technol. 2026;118(1).
35. Meng F, Fang B, Han Y, Song B, Wang Y, Wei Y. Spinel $MnFe_2O_4$-anchored biochar for robust peroxymonosulfate activation: Efficient Bisphenol A degradation with mechanistic insights and practical application. Journal of Water Process Engineering. 2026;81:109328.
36. Narayanaswamy V, Muralee Gopi CVV, Alzahmi S, Mahmoud ST, Issa B, Obaidat IM. Hierarchical battery-type $MnFe_2O_4$@$Ni(OH)_2$ spinel ferrite–hydroxide nanostructures for high-performance supercapacitors. Physical Chemistry Chemical Physics. 2026;28(24):14442-14454.
37. Raoof SA, Ahmed FJ, MO AB, Saleh MY. Synthesis, characterization, and biological activity of chromium complexes as efficient and novel catalysts for direct synthesis of carbonyl compounds from benzyl/cycloalkyl bromides in water under aerobic oxidation.
38. Zainab JM, Sahira K, Al-Abboodi AK, Alsaady HA. Enhancing Pediculicidal Activity Against Pediculus humanus capitis Using Iron Oxide Nanoparticle-Based Formulations of some Plant Extracts and Acetic Acid Solution. Nigerian Journal of Parasitology. 2024;45(2):460-469.
39. Al-Abboodi A, Falih IQ, Al-Asadi M, Hussein BA, Al-Saady MAAJ, Abdullah TA, et al. Iron-oxide nanoparticles (SPIONs) enhance malaria vaccine antibody response. Vaccine. 2026;77:128353.
40. ASSOCIATIONS. Chemical and Engineering News Archive. 1968;46(53):74-78.
41. Al-Abboodi A, Mhouse Alsaady HA, Banoon SR, Al-Saady M. Conjugation strategies on functionalized iron oxide nanoparticles as a malaria vaccine delivery system. Bionatura. 2021;3(3):2009-2016.
42. Latief F, Arrosyid BH, Amalia R, Fahroji M, Ghariy G, Aryanto D, et al. Composition and Annealing Process Influence on Structure, Local Structure, Electrical, and Magnetic Properties of $MnFe_2O_4$. The Journal of Physical Chemistry C. 2025;129(35):15724-15735.
43. Al-Abboodi A, Albukhaty S, Sulaiman GM, Al-Saady MAAJ, Jabir MS, Abomughaid MM. Protein Conjugated Superparamagnetic Iron Oxide Nanoparticles for Efficient Vaccine Delivery Systems. Plasmonics. 2023;19(1):379-388.
44. Gurumoorthy M, Palani G, Trilaksanna H, Kumar M. The structural, morphological, optical, thermal and magnetic properties of $MnFe_2O_4$ nanoparticles. Analytical Chemistry Letters. 2024;14(6):848-861.